Energy conversion theorems for some linear steady–states

L. A. Arias–Hernandez,[*] G. Valencia–Ortega,[†] and F. Angulo–Brown[‡]

Departamento de Física, Escuela Superior de Física y Matemáticas,

Instituto Politécnico Nacional, U. P. Zacatenco,

Edif. 9, 2o Piso, Ciudad de México, 07738, México.

C. R. Martinez–Garcia[§]

Departamento de Ciencias Básicas, Escuela Superior de Cómputo,

Instituto Politécnico Nacional, Av. Miguel Bernard,

Esq. Av. Miguel Othón de Mendizabal,

Colonia Lindavista, Ciudad de México 07738, México.

Abstract

One of the main issues that real energy converters present, when they produce effective work, is the inevitable entropy production. Within the context of Non-equilibrium Thermodynamics, entropy production tends to energetically degrade man-made or living systems. On the other hand, it is also not useful to think about designing an energy converter that works in the so-called minimum entropy production regime since the effective power output and efficiency are zero. In this manuscript, we establish some *Energy Conversion Theorems* analogous to Prigogine's one, their purpose is to reveal trade-offs between design and the so-called operation modes for (2×2)– linear isothermal energy converters. The objective functions that give rise to those thermodynamic constraints show stability. A two-meshes electric circuit was built as an example to demonstrate the Theorems' validity. Likewise, we reveal a type of energetic hierarchy for power output, efficiency and dissipation function when the circuit is tuned to any of the operating regimes studied here: maximum power output (MPO), maximum efficient power ($MP\eta$), maximum omega function ($M\Omega$), maximum ecological function (MEF), maximum efficiency ($M\eta$) and minimum dissipation function (mdf).

---

[*] larias@ipn.mx

I. INTRODUCTION

Since Prigogine formulated his principle of minimum entropy production in 1947 [1], also known as Prigogine's theorem, it has been subject to several controversies [2–7]. This theorem states that in the linear regime, where the Onsager reciprocal relations are valid [8], all steady states are characterized by the following extremum principle, *"...in the linear regime, the total entropy production in a system subject to flow of energy and matter reaches a minimum value at the non-equilibrium stationary state..."* [9]. Despite the criticism received, the Prigogine's theorem has prevailed mainly due to its experimental verifications; for example, in case of heat conduction in metallic rods [10, 11], as well as computer simulations of the same system [12].

In this last article, to demonstrate the validity of Prigogine's theorem, Lurié and Wagensberg took as the only fixed force, the following temperature gradient $F_0 = T_h^{-1} - T_0^{-1}$, i.e, it considers extreme thermal reservoir temperatures of the rod. The rest of the $(n-1)$ slices temperatures of their discrete model are used to construct the free forces F_k, for $k = 1, 2, ..., (n-1)$. Under this assumption, they arrive to the minimum entropy production regime by following all the steps of the Prigogine procedure. It is important to note that in [12], the so-called phenomenological coefficients L were used to represent the Fourier Law in the unidimensional form $J(x,t) = LX(x,t)$, where $L = kT^2$. That is, the thermal conductivity depends on T^{-2} and as was asserted by Jaynes [3], there is no known substance which obeys this relation. This obstacle was surrounded by Lurié and Wagensberg by considering that for small enough temperature gradients the effects of taking $L = kT^2$ are not important. This claim works reasonably. However, in [9] by means of the Euler-Lagrange formalism, the authors arrive at the function $T(x)$, which minimizes the entropy production and is also linear with respect to x-variable, by taking $L = kT^2 \approx kT_{av}^2$, where T_{av} is the average temperature of the rod. If the temperature gradient is small enough in the rod one will have that $T(x) = T_{av}[1 + \varepsilon(x)]$ with $|\varepsilon(x)| \ll 1$ [4]. For example, in [11] the corresponding experiment was performed for $\Delta T = 341.5\text{K} - 250\text{K} = 51.5\text{K}$ and for each case $|\varepsilon(x)| \sim 10^{-4}$ and the above-mentioned approximation is hold. Another strong support in favor of Prigogine's theorem in [13], is that Klein and Meijer proved it by using statistical

[†] gvalenciao1600@alumno.ipn.mx

[‡] fangulob@ipn.mx

[§] cemartinezg@ipn.mx

2

mechanics methods. They assumed a process consisting of mass and energy fluxes through a narrow tube that in turn connect two containers of an ideal gas. Such as occurs when a gas is enclosed by rigid adiabatic walls, which at the same time is connected by means of a diathermic piston with a reservoir of both temperature and pressure, this type of systems reach the final equilibrium state with their respective reservoirs without performing work. Something analogous happens in processes towards the steady state described in the previous heat conduction examples. In the case of the aforementioned gas interacting with the temperature and pressure reservoir, and by using the concept of thermodynamic availability and coupling with a second system give rise to the maximum useful work theorem [14, 15]. Similarly, within the context of Linear Irreversible Thermodynamics (LIT), a large number of steady states arise from the coupling of spontaneous processes and non-spontaneous ones. These couplings can exist in both living and man-made systems. Remarkably, this coupling concept can lead to energy conversion processes [16–18]. Caplan and Essig [17] developed a theory based on LIT for the study of linear biologic energy converters, that work in steady states. These authors introduced concepts such as power output and efficiency with the purpose to optimize the energy conversion process. Likewise, they took the usual notion of entropy production. Later, Stucki [16] used those ideas in the analysis of oxidative phosphorylation to establish other working regimes different than the minimum entropy production. In addition, Arias-Hernandez et al [18] used concepts from Finite-Time Thermodynamics to analyse the above-mentioned process. It is clear that in heat conduction experiments subjected to small temperature gradients, the systems evolves towards a steady final state of minimal entropy production. Yet, as several authors have been shown [16–20], in the case of two or more coupled processes, there are other steady states where certain quantity of interest to be optimized may come from natural or artificial needs.

The foregoing can translate into different proposal of trade-offs through characteristic functions, which are described in Section 2 of this article, i.e, thermodynamic mechanisms can be assumed whose goals are to maximize some energetic objective functions. Thus, at least five analogous of Prigogine's theorem can be stated (Section 3), whose purpose is to show physical restrictions for (2×2)–linear isothermal energy converters to operate in some optimal and stable regimes. In Section 4, we design a two-mesh electrical circuit to exhibit nonzero energy conversion when the coupling of electrical currents meet the physical constraints imposed by these types of "Energy Conversion Theorems" and experimental

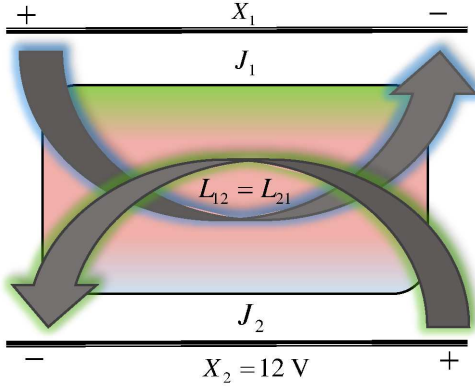FIG. 1. Sketch of a simple isothermal energy converter (2 coupled fluxes promoted by 2 conjugated forces), where $X_1 < 0$ is the force associated with the non-spontaneous flux, while $X_2 > 0$ is the another one related to the spontaneous flux.

verification thereof is presented. Finally, our conclusions are exposed in Section 5.

II. STEADY STATES WITHOUT MINIMUM ENTROPY PRODUCTION

Several phenomena in nature that are related to the transport of mass, charge and energy have been described with a good approximation in the linear regime [8, 21–23]. In general, the characteristic functions, that have been defined to study non-equilibrium processes in a variety of man-made and living systems, can be expressed in terms of sums of conjugate fluxes (J_i's) and forces (X_i's) [16–20, 24, 25]. Every J_i's are the so-called thermodynamic fluxes, such as the strain rate, reaction speed, electrical current, rate of muscle contraction, etc. The X_i's are defined as the thermodynamic forces, such as the stress tensor, reaction affinities, electrochemical potential muscle tension, etc.

Most of the previous simple linear relations are well-known, for example, Ohm's Law for electrical current, Fick's Law for diffusion, Fourier Law for heat flow, etc. The main feature of these uncoupled processes is their apparent contribution to the increase of system's entropy and a decrease in its free energy, i.e, the associated fluxes with these processes are spontaneous. However, there are other cases, characterized by multiple interacting fluxes. This type of processes involve an energy transfer, which can be considered of two parts: the one associated with an entropy increase and the other one with a decrease of entropy [18, 26–28]. To illustrate it, we can take as an example the transport of an ion across a cell

4

membrane, which may be influenced not only by its electrochemical gradient, but also by the influence of other gradient, such as a external pressure.

In order to characterize a type of processes that occur in open thermodynamic systems is through the so-called steady states. These steady states are typical of systems whose processes are kept constant on time, so the entropy created by the steady flow is more relevant than the entropy transferred to the surroundings [17, 20, 29, 30],

$$\frac{dS_T}{dt} = \frac{dS_{int}}{dt} + \frac{dS_{ext}}{dt} > 0, \tag{1}$$

where $\dot{S}_{int} \equiv \sigma = \hat{J} : \hat{X}$ is usually called the entropy production while $\dot{S}_{ext} = 0$, since the entropy flux from the surroundings is equal to the entropy flux toward the system. That is, internal irreversibilities are responsible for the total entropy increments of the thermodynamic universe.

In the case of (2×2)–isothermal linear energy converter models, the entropy production is also a positive semidefinite quadratic form [8, 9, 17, 18, 20, 21, 26, 31]:

$$\begin{aligned} \sigma &= J_1 X_1 + J_2 X_2 \\ &= [X_1, X_2] \begin{bmatrix} L_{11} & q\sqrt{L_{11}L_{22}} \\ q\sqrt{L_{11}L_{22}} & L_{22} \end{bmatrix} \begin{bmatrix} X_1 \\ X_2 \end{bmatrix} > 0, \end{aligned} \tag{2}$$

where the coefficient matrix $\hat{L}$ is symmetric, and the so-called coupling coefficient $q = L_{12}/\sqrt{L_{11}L_{22}}$ fulfills that $q^2 \in [0,1]$, with $L_{11} > 0$ and $L_{22} > 0$. Since the purpose of those models is energy conversion, three energetic functions (process variables) with extreme conditions can be defined, the dissipation function ($\Phi \equiv T\sigma$), power output ($P_O \equiv -TJ_1X_1$) and efficiency ($\eta \equiv P_O/P_I = -TJ_1X_1/TJ_2X_2$),

$$\Phi = \left(x^2 + 2qx + 1\right) TL_{22}X_2^2 \tag{3a}$$

$$P_O = -x\left(x + q\right) TL_{22}X_2^2 \tag{3b}$$

$$\eta = -\frac{(x + q)\, x}{qx + 1}, \tag{3c}$$

here we introduce a performance parameter $x = \sqrt{L_{11}/L_{22}} X_1/X_2$, called the force ratio [42]. It measures the cross effect between two potentials [17, 18].
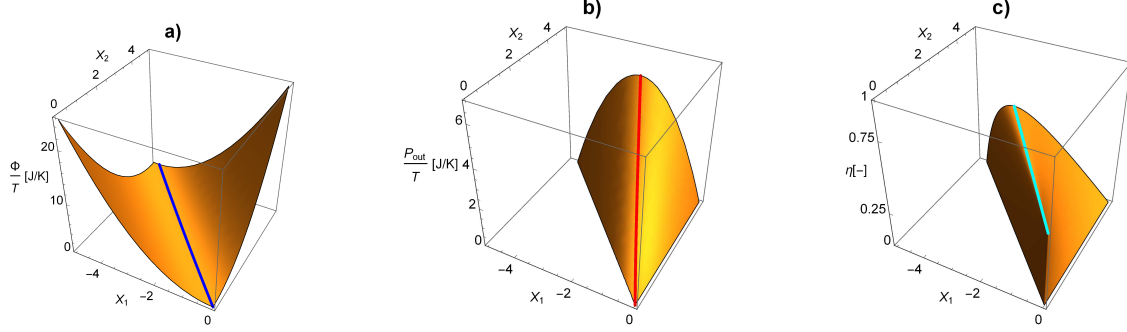
5

FIG. 2. Energetic functions versus X_1 (driven force) and X_2 (driver force) for an isothermal linear energy converter. Normalized dissipation function (a), normalized power output (b) and efficiency (c), all of them are plotted for a fixed value of $q = 0.97$. They reach their extreme values at $X_1^{mdf} = -\sqrt{L_{22}/L_{11}}\, X_2\, q$ (blue line), $X_1^{MPO} = -\sqrt{L_{22}/L_{11}}\, X_2\, q/2$ (red line) and $X_1^{M\eta} = -\sqrt{L_{22}/L_{11}}\, X_2\, q/\left(1+\sqrt{1-q^2}\right)$ (cyan line), respectively.

Under this linear energy converters scheme (see Fig. 1) [17, 18, 23], X_1 can be defined as the driven force while X_2 as the driver force, that is, $X_1 = X_1(q, X_2)$. Fig 2 shows the extremes in the three functions (Φ, P_O and η) at different values of (X_1, X_2), and at the same time, they are associated to three different operation modes, the minimum dissipation function (mdf), maximum power output (MPO) and maximum efficiency ($M\eta$). The optimal values that x adopts for each of the process variables in Eq 2 are:

$$x^{mdf} = -q \tag{4a}$$

$$x^{MPO} = -\frac{q}{2}, \tag{4b}$$

$$x^{M\eta} = -\frac{q}{1 + \sqrt{1 - q^2}}; \tag{4c}$$

consequently, other objective functions express different trade–offs between the energetic functions Φ, P_O and η can be defined, therefore they also have extreme values (see Fig. 3). The objective functions that we will study to characterize their optimal operation modes are [16, 20, 32]:

$$E_F = -\left(2x^2 + 3xq + 1\right) T L_{22} X_2^2 \tag{5a}$$

$$\Omega = \left[\eta_M\left(qx + 1\right) - 2x\left(x + q\right)\right] T L_{22} X_2^2 \tag{5b}$$

$$P_\eta = \frac{\left[(x + q)\, x\right]^2}{qx + 1} T L_{22} X_2^2, \tag{5c}$$
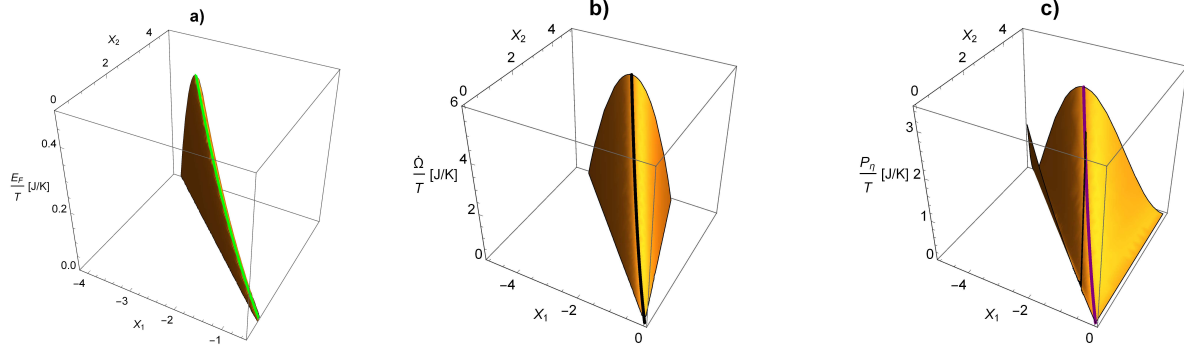
6

FIG. 3. Objective functions versus X_1 (driven force) and X_2 (driver force) for an isothermal linear energy converter. Normalized ecological function (a), normalized omega function (b) and normalized efficient power (c), all of them are plotted for a fixed value of $q = 0.97$. They reach their extreme values at X_1^{MEF} (green line), $X_1^{M\Omega}$ (black line) and $X_1^{MP\eta}$ (purple line), respectively.

where $E_F = P_O - \Phi$ is the ecological function [33], $\Omega = (2 - {}^{\eta_M}/_\eta)\, P_O$ is the so–called omega [32], with η_M the value of efficiency under the conditions that maximize it, i.e., Eq. 3c evaluated at Eq. 4c, and $P\eta = \eta P_O$ is the efficient power [16, 34]. Each of the previous objective functions [Eqs. (3) and (5)] give us optimal performance modes, such as maximum ecological function (MEF), maximum Ω–function ($M\Omega$) and maximum efficient power ($MP\eta$), for a linear energy converter, and their optima x–values are,

$$x^{MEF} = -\frac{3q}{4} \tag{6a}$$

$$x^{M\Omega} = -\frac{q\left(4 - q^2 + 4\sqrt{1 - q^2}\right)}{4\left(1 + \sqrt{1 - q^2}\right)^2} \tag{6b}$$

$$x^{MP\eta} = -\frac{4 + q^2 - \sqrt{16 - 16q^2 + q^4}}{6q}. \tag{6c}$$

The above–mentioned physically accessible characteristic points can be viewed in a P_O vs. η plane (see Fig. 4 of [18]), in a similar way to the behavior of heat engines that operate in cycles between two thermal reservoirs [18, 35].

A. Optimal performance modes within Φ vs. η and P_O vs. η spaces

In describing the performance of a linear energy converter, the process variables can define a configuration space to display all physically possible realizations. Then, $\Phi = \Phi(\eta)$ and

$P_O = P_O(\eta)$, this parametric way of representing the dissipation and the power output of a linear energy converter, for $q \in [q_{min}, 1]$, allows us to note that the dissipation function has an inverse decreasing monotonous behavior, that is, when q decreases the limit value of Φ increases while η diminishes [18]. From the parametric graphs depicted in [18, 28, 36, 37], we can observe that when the quality of the coupling between spontaneous and non-spontaneous fluxes is low, entropy production increases. On the other side, the well-known loop–shaped curves for heat engines [38] arise in LIT energy converters when $P_O = P_O(\eta, q)$. These loops intrinsically show the existence of extra–thermodynamic conditions that dynamically constrain the processes of a linear energy converter. Each loop has two optimal points of interest [18, 28], the one that corresponds to maxima P_O points and the other one to maximum-η points, between these two points the other performance regimes can be achieved [39]. This zone reveals energy conversion with high power output, high efficiency, and low dissipated energy.

When the operation modes associated with the three trade-off functions, are evaluated in the so-called process variables (Φ, P_O, η) the following hierarchies are established (see Appendix A),

$$\Phi_{mdf} < \Phi_{M\eta} < \Phi_{MEF} < \Phi_{M\Omega} < \Phi_{MP\eta} < \Phi_{MPO} \tag{7a}$$

$$P_O^{mdf} < P_O^{M\eta} < P_O^{MEF} < P_O^{M\Omega} < P_O^{MP\eta} < P_O^{MPO} \tag{7b}$$

$$\eta_{mdf} < \eta_{MPO} < \eta_{MP\eta} < \eta_{M\Omega} < \eta_{MEF} < \eta_{M\eta} \tag{7c}$$

The infinite optimal performance regimes located between $\left[P_O^{MPO}, P_O^{M\eta} \right]$ can be achieved when the flux associated with the driven force is tuned by means of the coupling coefficient with the flux associated with the driver force. That is, operation modes are linked with objective functions, which in principle can be built through the process variables.

III. ENERGY CONVERSION THEOREMS FOR SOME LINEAR STEADY–STATES

In general, the validity limits for the hypotheses of LIT can be experimentally verified, using several non-equilibrium systems characterized by continuous variables [9, 11, 40, 41]. In particular, the Onsager relations have been shown to reflect the experimental results for small thermodynamic gradients, that is, the postulates of LIT are valid in situations close to a steady state [8, 9, 21, 29, 30].

In systems whose coupled processes are promoted by constant and free thermodynamic forces, the entropy production will always adapt to a condition in which the associated steady state causes the same systems to dissipate the least energy possible to the surroundings (minimum entropy production regime) [9, 25, 29, 30]. On the other side, energy converters open up a range of physically accessible steady states, which represent thermodynamic constraints under boundary conditions that correspond to optimal operating criteria [16, 18–20, 26, 27]. These processes are characterized by a set of free fixed forces ($X_i > 0$) and another set of constant forces ($X_j < 0$) but subject to an external condition.

For the case of energy converters with two forces and two coupled fluxes, the principle of minimum entropy production can be claimed in terms of the dissipation function (Φ). This new rewritten form can be stated as the minimum dissipation function **mdf–THEOREM**, as follows [31, 36]:

(**mfd–THEOREM**). *When a non equilibrium steady–state system is characterized by two generalized forces X_1 (the one associated with driven processes) and X_2 (another one associated with driver processes), it is driven to a steady state when the driver force is fixed. Then, under the condition of **minimum dissipation function**, the J_1 flux is equal to 0.*

Proof. Let us take the mathematical expression for dissipation function [Eq. (2)]. By calculating the derivative of Φ with respect to X_1 assuming X_2 fixed, we obtain:

$$\left(\frac{\partial \Phi}{\partial X_1}\right)_{X_2} = T\left[J_1 + L_{11}X_1 + q\left(\sqrt{L_{11}L_{22}}\right)X_2\right]. \tag{8}$$

By hypothesis $\left(\frac{\partial \Phi}{\partial X_1}\right)_{X_2} = 0$; therefore:

$$J_1 = 0. \tag{9}$$

QED

In order to establish a trade–off between design and operation mode of a linear energy converter, we will set out the following corollary that results from canceling the driven process.

(*mdf*–**COROLLARY**). *If the degree of coupling between the processes of a non equilibrium steady–state system is measured by the parameter q and it is also operating under the **mfd** regime, the cross effect between both generalized forces, denoted by the parameter x, is given by $x = -q$.*

Proof. From the mdf–**THEOREM**, the constraint $J_1 = 0$ lead us to write the force X_1 as:

$$X_1 = -q\left(\sqrt{\frac{L_{22}}{L_{11}}}X_2\right). \tag{10}$$

By using the definition for x, we obtain

$$x = -q. \tag{11}$$

QED

The steady states that can be identified within a linear energy converter correspond to the coupling of two observable processes, the so–called spontaneous and other non-spontaneous. This distinction was not fully identified by Prigogine, since in his minimum entropy production principle statement, he made no distinction about the entropic nature of thermodynamic forces promoting coupled fluxes. Likewise, we intrinsically show by means of a simple step that minimum dissipation theorem is the energetic version of minimum entropy production principle. In fact, each of the optimization criteria presented in Section 2 satisfies a variational principle and can be represented by specific flux–force relations [43, 44]. Thus, energy conversion processes can be associated with different stationary solutions. When the operation modes coincide, their steady states are adjusted to one under the same initial condition (the same degree of coupling q).

A. Analogous theorems to the minimum entropy production for (2×2)–energy converters

As we have evidenced in Section 2, in a large number of non equilibrium steady–state processes that are carried out in both living and man–made systems, appropriate constrains (boundary conditions) can be found so that the energy transfer takes place in particular operation modes. If the purpose in the operation of a (2×2)–isothermal linear energy converter is not to minimize the entropy production, the steady states that dynamically constrain the processes within the converter in the optimal performance regimes (MPO, $M\eta$, MEF, $M\Omega$ and $MP\eta$) [16, 20, 23, 32, 45], steady states revealed through the energy conversion theorems analogous to the Prigogine one (**mfd–THEOREM**), as well as their corresponding corollaries. The optimal regimes here analyzed were taken from the field of Finite Time Thermodynamics (FTT) [18, 46].

(*MPO*–**THEOREM**). *When a non equilibrium steady–state system is characterized by two generalized forces X_1 (the one associated with driven processes) and X_2 (another one associated with driver processes), it is arrested at a steady state when the driver force is fixed. Then, under the condition of **maximum power output**, the J_1 flux is equal to $-L_{11}X_1$.*

Proof. Let us consider the mathematical expression for power output [Eq. (3)]. The partial derivative of P_{out} with respect to X_1 assuming X_2 fixed, is:

$$\left(\frac{\partial P_O}{\partial X_1}\right)_{X_2} = -T\left(J_1 + L_{11}X_1\right). \tag{12}$$

By hypothesis $\left(\frac{\partial P_O}{\partial X_1}\right)_{X_2} = 0$, we get:

$$J_1 = -L_{11}X_1. \tag{13}$$

QED

(*MPO*–**COROLLARY**). *If the degree of coupling between the processes of a non equilibrium steady–state system is measured by the parameter q and it is also operating under the **MPO** regime, the cross effect between both generalized forces, denoted by the parameter x, is given by $x = -\frac{q}{2}$.*

Proof. From the *MPO*–**THEOREM**, the constraint $J_1 = -L_{11}X_1$ lead us to write the force X_1 as:

$$X_1 = -\frac{q}{2}\left(\sqrt{\frac{L_{22}}{L_{11}}}X_2\right). \tag{14}$$

By using the definition for x, we have

$$x = -\frac{q}{2}. \tag{15}$$

QED

(*Mη*–**THEOREM**). *When a non equilibrium steady–state system is characterized by two generalized forces X_1 (the one associated with driven processes) and X_2 (another one associated with driver processes), it is arrested at a steady state when the driver force is fixed. Then, under the condition of **maximum efficiency**, the J_1 flux is equal to $-\left(\frac{1-\eta}{1+\eta}\right)L_{11}X_1$.*

11

Proof. Let us take the mathematical expression for efficiency [Eq. (3)]. By calculating the partial derivative with respect to X_1 assuming X_2 fixed, we obtain

$$\left(\frac{\partial \eta}{\partial X_1}\right)_{X_2} = -\frac{P_O}{P_I^2}\left(\frac{\partial P_I}{\partial X_1}\right) + \frac{1}{P_I}\left(\frac{\partial P_O}{\partial X_1}\right), \tag{16}$$

where P_I is the rate of incoming energy per temperature unit, this amount of energy is associated with spontaneous flux. The derivative $\left(\frac{\partial P_O}{\partial X_1}\right)$ is given in MPO–**THEOREM**, while $\left(\frac{\partial P_I}{\partial X_1}\right)$ is:

$$\left(\frac{\partial P_I}{\partial X_1}\right) = Tq\sqrt{L_{11}L_{22}}X_2. \tag{17}$$

Then, we can rewrite $\left(\frac{\partial \eta}{\partial X_1}\right)_{X_2}$ as follows:

$$\left(\frac{\partial \eta}{\partial X_1}\right)_{X_2} = -\frac{T}{P_I}\left[\frac{P_O}{P_I}q\sqrt{L_{11}L_{22}}X_2 + J_1 + L_{11}X_1\right]. \tag{18}$$

By hypothesis $\left(\frac{\partial \eta}{\partial X_1}\right)_{X_2} = 0$ and, by using the definition of η, we get:

$$\eta\left(q\sqrt{L_{11}L_{22}}X_2 + L_{11}X_1 - L_{11}X_1\right) + J_1 + L_{11}X_1 = 0. \tag{19}$$

Finally,

$$J_1 = -\left(\frac{1-\eta}{1+\eta}\right)L_{11}X_1. \tag{20}$$

QED

($M\eta$–**COROLLARY**). *If the degree of coupling between the processes of a non equilibrium steady–state system is measured by the parameter q and it is also operating under the $M\eta$ regime, the cross effect between both generalized forces, denoted by the parameter x, is given by $x = -\frac{q}{1+\sqrt{1-q^2}}$.*

Proof. From the $M\eta$–**THEOREM**, the constraint $J_1 = -\left(\frac{1-\eta}{1+\eta}\right)L_{11}X_1$ lead us to write the force X_1 as:

$$X_1 = -\frac{q(1+\eta)}{2}\left(\sqrt{\frac{L_{22}}{L_{11}}}X_2\right). \tag{21}$$

By using the definition for x, as well as Eq.3c, we have

$$x = -\frac{q}{1+\sqrt{1-q^2}}. \tag{22}$$

QED

(MEF–**THEOREM**). *When a non equilibrium steady–state system is characterized by two generalized forces X_1 (the one associated with driven processes) and X_2 (another one associated with driver processes), it is arrested at a steady state when the driver force is fixed. Then, under the condition of **maximum ecological function**, the J_1 flux is equal to $-\frac{1}{3}L_{11}X_1$.*

Proof. Let us consider the mathematical expression for the so-called ecological function [Eq. (5a)]. The partial derivative with respect to X_1 assuming X_2 fixed, is:

$$\left(\frac{\partial E_F}{\partial X_1}\right)_{X_2} = -T\left(J_1 + L_{11}X_1 + 2J_1\right). \tag{23}$$

By hypothesis $\left(\frac{\partial E_F}{\partial X_1}\right)_{X2} = 0$, we get

$$J_1 = -\frac{1}{3}L_{11}X_1. \tag{24}$$

QED

(MEF–**COROLLARY**). *If the degree of coupling between the processes of a non equilibrium steady–state system is measured by the parameter q and it is also operating under the **MEF** regime, the cross effect between both generalized forces, denoted by the parameter x, is given by $x = -\frac{3q}{4}$.*

Proof. From the MEF–**THEOREM**, the constraint $J_1 = -\frac{1}{3}L_{11}X_1$ lead us to write the force X_1 as:

$$X_1 = -\frac{3q}{4}\left(\frac{L_{22}}{L_{11}}X_2\right). \tag{25}$$

By using the definition for x, we have

$$x = -\frac{3q}{4}. \tag{26}$$

QED

($M\Omega$–**THEOREM**). *When a non equilibrium steady–state system is characterized by two generalized forces X_1 (the one associated with driven processes) and X_2 (another one associated with driver processes), it is arrested at a steady state when the driver force is fixed. Then, under the condition of **maximum omega function**, the J_1 flux is equal to $-\left(\frac{2-\eta_M}{2+\eta_M}\right)L_{11}X_1$.*

13

Proof. Let us take the mathematical expression for the so-called omega function [Eq. (5b)]. By calculating the partial derivative of Ω with respect to X_1 and by assuming X_2 fixed,

$$\left(\frac{\partial \Omega}{\partial X_1}\right)_{X_2} = -T\left[(2 + \eta_M) J_1 + (2 - \eta_M) L_{11} X_1\right]. \tag{27}$$

By hypothesis $\left(\frac{\partial \Omega}{\partial X_1}\right)_{X_2} = 0$. Then, we obtain

$$J_1 = -\left(\frac{2 - \eta_M}{2 + \eta_M}\right) L_{11} X_1. \tag{28}$$

QED

($M\Omega$–**COROLLARY**). *If the degree of coupling between the processes of a non equilibrium steady–state system is measured by the parameter q and it is also operating under the $M\Omega$ regime, the cross effect between both generalized forces, denoted by the parameter x, is given by $x = -\frac{q\left(4 - q^2 + 4\sqrt{1-q^2}\right)}{4\left(1 + \sqrt{1-q^2}\right)^2}$.*

Proof. From the $M\Omega$–**THEOREM**, the constraint $J_1 = -\left(\frac{2-\eta_M}{2+\eta_M}\right) L_{11} X_1$ lead us to write the force X_1 as:

$$X_1 = -\frac{q(2 + \eta_M)}{4}\left(\sqrt{\frac{L_{22}}{L_{11}}} X_2\right), \tag{29}$$

by using the definition for x and $\eta_M = \eta\left(x^{M\eta}, q\right)$, we obtain

$$x = -\frac{q\left(4 - q^2 + 4\sqrt{1 - q^2}\right)}{4\left(1 + \sqrt{1 - q^2}\right)^2}. \tag{30}$$

QED

($MP\eta$–**THEOREM**). *When a non equilibrium steady–state system is characterized by two generalized forces X_1 (the one associated with driven processes) and X_2 (another one associated with driver processes), it is arrested at a steady state when the driver force is fixed. Then, under the condition of **maximum efficient power**, the J_1 flux is equal to $-\left(\frac{2-\eta}{2+\eta}\right) L_{11} X_1$.*

Proof. Let us consider the mathematical expression for the so-called efficient power [Eq. (5c)]. By calculating the partial derivative of P_η with respect to X_1 assuming X_2 fixed,

$$\left(\frac{\partial P_\eta}{\partial X_1}\right)_{X_2} = -\frac{T P_{out}}{P_{in}}\left[\frac{P_{out}}{P_{in}} L_{12} X_2 + 2\left(J_1 + L_{11} X_1\right)\right]. \tag{31}$$

14

By hypothesis $\left(\frac{\partial P_\eta}{\partial X_1}\right)_{X_2} = 0$ and by using the definition of η, we have

$$2J_1 + 2L_{11}X_1 + \eta\left(L_{12}X_2 + L_{11}X_1 - L_{11}X_1\right) = 0. \tag{32}$$

Finally,

$$J_1 = -\frac{2-\eta}{2+\eta}L_{11}X_1. \tag{33}$$

QED

($MP\eta$–**COROLLARY**). *If the degree of coupling between the processes of a non equilibrium steady–state system is measured by the parameter q and it is also operating under the $MP\eta$ regime, the cross effect between both generalized forces, denoted by the parameter x, is given by $x = -\frac{4+q^2-\sqrt{q^4-16q^2+16}}{6q}$.*

Proof. From the **MPη–THEOREM**, the constraint $J_1 = -\frac{2-\eta}{2+\eta}L_{11}X_1$ lead us to write the force X_1 as:

$$X_1 = -\frac{q\left(2+\eta\right)}{4}\left(\sqrt{\frac{L_{22}}{L_{11}}}X_2\right). \tag{34}$$

By using the definitions for x and η, we get

$$x = -\frac{4+q^2 - \sqrt{q^4 - 16q^2 + 16}}{6q}. \tag{35}$$

QED

As has been pointed out in some works [47, 48], a boundary condition that at the same time is linked to a particular dynamic performance mode has several stable steady solutions. The energetic optimization criteria presented in Section 2 can be equivalent when the degree of coupling between the flows adopt particular values. For instance, the steady state associated with the minimum dissipation function condition is identical to the other extreme criteria, in Table I the values of q are displayed. Other constraints can also be established using the previous corollaries and evaluating q in the characteristic functions presented in Section 2.

All of the above energetic trade–offs fulfill the condition $\Phi > 0$, since the non-equilibrium steady states associated with them, only appear when external thermodynamic forces are linked under an extreme condition. Thus, the operation modes involve the maintenance of steady states for coupled processes that waste free energy at different rates.

15

TABLE I. Physical constraints on linear energy converters so that two or more steady states coincide with the minimum dissipation function condition.

Boundary Conditions	q
$\Phi_{mdf}(q) = \Phi_{MPO}(q)$	0
$\Phi_{mdf}(q) = \Phi_{M\eta}(q)$	0 and 1
$\Phi_{mdf}(q) = \Phi_{MEF}(q)$	0
$\Phi_{mdf}(q) = \Phi_{M\Omega}(q)$	0
$\Phi_{mdf}(q) = \Phi_{MP\eta}(q)$	0

B. Temporal evolution of the characteristic functions and stability of their steady states

The analysis of external perturbations on different types of thermal cycle models has been topic of interest [49–52]. Since thermal engines operate with many cycles per unit time, the effect of noisy perturbations has been able to help to have a well-design systems guaranteeing stability in their operating regimes (steady-state regimes) [53–55]. In several analysis on LIT [9, 29, 56–58], it has been shown that spontaneous fluctuations on a particular steady state drive the system back to its condition of *minimum entropy production*. For the case of a (2×2)-isothermal energy converters, let us consider the dissipation function $\Phi = \Phi(X_i, J_i)$ in a non-equilibrium steady state. As $\Phi = T \int_V (J_1 X_1 + J_2 X_2) \, dV$, the time variation of Φ can be written as:

$$
\begin{aligned}
\frac{d\Phi}{dt} &= \int_V \left(J_1 \frac{dX_1}{dt} + J_2 \frac{dX_2}{dt} \right) dV + \\
&\quad \int_V \left(X_1 \frac{dJ_1}{dt} + X_2 \frac{dJ_2}{dt} \right) dV \\
&\equiv \frac{d_X \Phi}{dt} + \frac{d_J \Phi}{dt},
\end{aligned} \tag{36}
$$

where $d_X\Phi/dt$ is the time variation of spontaneous and non-spontaneous thermodynamic forces and $d_J\Phi/dt$ is the temporal change of the conjugated fluxes. In the linear regime a general property has been stated [9, 29, 56]:

$$
\frac{d_X \Phi}{dt} = \frac{d_J \Phi}{dt}. \tag{37}
$$

If we assume hereinafter homogeneity and unitary volume, the time derivative of each X_i

can be written by noting that

$$\frac{dX_i}{dt} = \sum_k \left(\frac{\partial X_i}{\partial a_k}\right) \frac{da_k}{dt}. \tag{38}$$

Thus, we find

$$\frac{d\Phi}{dt} = 2T \left[J_1 \sum_{k=1}^{2} \left(\frac{\partial X_1}{\partial a_k}\right) J_k + J_2 \sum_{k=1}^{2} \left(\frac{\partial X_2}{\partial a_k}\right) J_k \right], \tag{39}$$

where Onsager reciprocal relations and the definition of $da_k/dt \equiv J_k$ have been considered. On the other side, since the LIT has been constructed using the so–called Local Equilibrium Hypothesis [8, 31], in a neighborhood of the equilibrium state, $\partial X_i/\partial a_k$ would retain its negative definiteness for the spontaneous terms, while non-spontaneous ones are positive. In addition, because of $X_1 < 0$ and $X_2 > 0$. Hence, in this neighborhood we have

$$\frac{d\Phi}{dt} < 0. \tag{40}$$

This condition ensures the stability of the steady state associated with the dissipation function, since in general the magnitude of the direct effects are greater than the cross effects.

1. Power output temporal evolution

In the same way, given an arbitrary volume, let us now consider the power output for a (2×2)-isothermal energy converter $P_O = P_O(X_i, J_i)$. Then, the time variation of P_O is

$$\frac{dP_O}{dt} \equiv - \left(\frac{d_X P_O}{dt} + \frac{d_J P_O}{dt} \right), \tag{41}$$

under the same mathematical assumptions of [9, 29, 56],

$$\frac{d_J P_O}{dt} < \frac{d_X P_O}{dt}, \tag{42}$$

and by using the condition given by Eq. (38). We have:

$$\frac{dP_O}{dt} = -T \left[(J_1 + L_{11}X_1) \sum_{k=1}^{2} \left(\frac{\partial X_1}{\partial a_k}\right) J_k + \right.$$

$$\left. (J_2 - L_{22}X_2) \sum_{k=1}^{2} \left(\frac{\partial X_2}{\partial a_k}\right) J_k \right]. \tag{43}$$

Therefore, in the neighborhood of the equilibrium state

$$\frac{dP_O}{dt} < 0, \tag{44}$$

since $|L_{11}X_1| < |L_{22}X_2|$. This new constrain guarantees the stability of a steady state linked to the power output regime.

2. Efficiency temporal evolution

For the case of the efficiency in this type of linear energy converters, $\eta = \eta(X_i, J_i)$. The temporal evolution of η can be written as

$$\frac{d\eta}{dt} \equiv -\frac{1}{P_I^2}\left[P_I\left(\frac{d_X P_O}{dt} + \frac{d_J P_O}{dt}\right) - P_O\left(\frac{d_X P_I}{dt} + \frac{d_J P_I}{dt}\right)\right]; \tag{45}$$

analogously, using the same mathematical constraints,

$$|P_O| < |P_I| \tag{46a}$$

$$\frac{d_X P_I}{dt} < \frac{d_J P_I}{dt}, \tag{46b}$$

and by considering Eq. (38),

$$\begin{aligned}
\frac{d\eta}{dt} = -\frac{1}{P_I^2}\Bigg[P_I\left(\frac{dP_O}{dt}\right) - \\
P_O\Bigg\{(J_1 - L_{11}X_1)\sum_{k=1}^{2}\left(\frac{\partial X_1}{\partial a_k}\right)J_k + \\
(J_2 + L_{22}X_2)\sum_{k=1}^{2}\left(\frac{\partial X_2}{\partial a_k}\right)J_k\Bigg\}\Bigg].
\end{aligned} \tag{47}$$

Hence, in the neighborhood of the equilibrium state:

$$\frac{d\eta}{dt} < 0, \tag{48}$$

where $|L_{11}X_1| < |L_{22}X_2|$ must be fulfilled. Once again, this new constraint describes the stability of a steady state related to this energetic function.

3. Temporal evolution of trade-off functions

Finally, let us take the mathematical expressions of the three objective functions: ecological function, omega function and efficient power; in order to analyze the effect of the fluctuations around their respective stable state.

a. Temporal evolution of E_F. For this (2×2)-linear system, $E_F = E_F(X_i, J_i)$ can be studied when it is disturbed,

$$\frac{dE_F}{dt} = -T\left[2\left(\frac{d_X P_O}{dt} + \frac{d_J P_O}{dt}\right) + \frac{d_X P_I}{dt} + \frac{d_J P_I}{dt}\right]. \tag{49}$$

18

From Eqs. (37) and (42), we can state that

$$\frac{d_J E_F}{dt} < \frac{d_X E_F}{dt},$$

(50)

and by using the definition of Eq. (38) as well as Eqs. (40) and (43),

$$\frac{dE_F}{dt} = -T\left[(3J_1 + L_{11}X_1)\sum_{k=1}^{2}\left(\frac{\partial X_1}{\partial a_k}\right)J_k + \right.$$

$$\left.(3J_2 - L_{22}X_2)\sum_{k=1}^{2}\left(\frac{\partial X_2}{\partial a_k}\right)J_k\right].$$

(51)

Then, in the vicinity of the equilibrium state,

$$\frac{dE_F}{dt} < 0.$$

(52)

$b.$ *Temporal evolution of Ω.*   Now, let us consider the omega function $\Omega = \Omega(X_i, J_i)$, its temporal variation is:

$$\frac{d\Omega}{dt} = -T\left[2\left(\frac{d_X P_O}{dt} + \frac{d_J P_O}{dt}\right) + \eta_M\left(\frac{d_X P_I}{dt} + \frac{d_J P_I}{dt}\right)\right].$$

(53)

Eqs. (37) and (42) allow us to establish that

$$\frac{d_J \Omega}{dt} < \frac{d_X \Omega}{dt},$$

(54)

then, taking the expressions given by Eqs. (38) and (43),

$$\frac{d\dot{\Omega}}{dt} = -T\left[\{(2 + \eta_M)J_1 + (2 - \eta_M)L_{11}X_1\}\sum_{k=1}^{2}\left(\frac{\partial X_1}{\partial a_k}\right)J_k + \right.$$

$$\left.\{(2 + \eta_M)J_2 - (2 - \eta_M)L_{22}X_2\}\sum_{k=1}^{2}\left(\frac{\partial X_2}{\partial a_k}\right)J_k\right].$$

(55)

Once again, in the zone near to the equilibrium state

$$\frac{d\Omega}{dt} < 0.$$

(56)

$c.$ *Temporal evolution of P_η.*   Finally, let us use the mathematical expression for the efficient power $P_\eta = P_\eta(X_i, J_i)$, the temporal evolution of this objective function is:

$$\frac{dP_\eta}{dt} = \frac{TP_O}{P_I^2}\left[2P_I\left(\frac{d_X P_O}{dt} + \frac{d_J P_O}{dt}\right) - P_O\left(\frac{d_X P_I}{dt} + \frac{d_J P_I}{dt}\right)\right].$$

(57)

Due to the validity of Eqs. (37) and (42), we can state that

$$\frac{d_J P_\eta}{dt} < \frac{d_X P_\eta}{dt},$$

(58)

19

by taking into account the constraints [Eqs. (43) and (46)], in the neighborhood of the equilibrium state:

$$\frac{dP_\eta}{dt} < 0. \tag{59}$$

Inequalities (51), (56) and (59) express new constraints that describe the stability of three steady states associated with three different objective functions.

The above-mentioned conditions ensure the stability of isothermal energy converters, whose energetic processes occur in the linear regime when small perturbations are considered. As the so-called characteristic functions are positive and also their respective temporal variation are negative, constitute the so-called Lyapunov conditions [57]. They guarantee the stability of any dynamic state, i.e, those states are considered simple attractors when the systems experience energetic fluctuations.

IV. AN APPLICATION OF ENERGY THEOREMS: ELECTRIC CIRCUIT WITH RESISTORS ELEMENTS AND TWO COUPLED FLUXES

In this section, we apply the previous results, associated with steady states without minimum entropy production, to study the energetics for a (2×2)–isothermal linear energy converter consisting of an electric circuit of two meshes with passive elements (resistors) and powered by two DC voltage sources (see Fig. 4). Through Kirchhoff's equations that describe the energy conservation between the meshes, within the context of generalized flows and forces, we found the so-called cross effect $(L_{12} = L_{21})$ is fulfilled. Then, from the parameters related to its design (q) and its operation modes (x), we can characterize all the optimal operating criteria that correspond to particular stationary states.

A. Dynamic equations of the resistive circuit

Let us consider the electric currents involved are time independent, with J_1 the driven flux that flows through the mesh 1 and J_2 the driver flux that gets about through the mesh 2. In addition, X_1 and X_2 are the DC voltage sources that promote the fluxes. As the circuit phenomenological equations can be associated with the Kirchhoff laws, then for the mesh 1 (left side in figure 4) we have,

$$X_1 = (R_1 + R_2) J_1 - R_2 J_2, \tag{60}$$

20
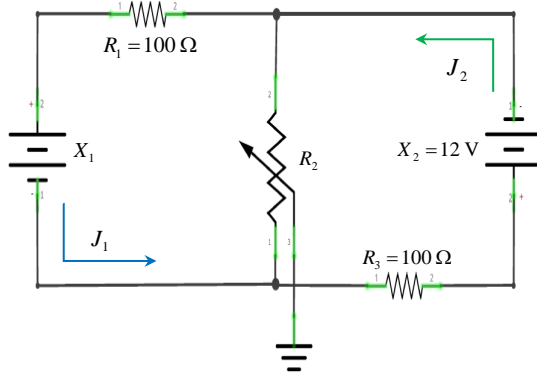
FIG. 4. Two-mesh resistive electric circuit, modeled as a (2×2)-simple isothermal energy converter. In this case, the voltage source X_1 is associated with the non-spontaneous flux J_1, while the fixed voltage source X_2 is related to the spontaneous flux J_2.

while for the mesh 2 (right side of Fig. 4),

$$X_2 = (R_2 + R_3) J_2 - R_2 J_1. \tag{61}$$

In order to study the phenomenological equation of this system in the Onsager context, we must reverse Eqs. (60) and (61), i.e, writing (J_1, J_2) in terms of (X_1, X_2). Hence,

$$\begin{pmatrix} J_1 \\ J_2 \end{pmatrix} = \begin{pmatrix} \frac{R_2+R_3}{\Delta} & \frac{R_2}{\Delta} \\ \frac{R_2}{\Delta} & \frac{R_1+R_2}{\Delta} \end{pmatrix} \begin{pmatrix} X_1' \\ X_2' \end{pmatrix}, \tag{62}$$

where $\Delta = R_1 (R_2 + R_3) + R_2 R_3$ and $X_{1,2}' = {}^{X_{1,2}}/_{T}$. As it can be noticed the equation system [Eq. (62)] is by itself the generalized Onsager equations whose equality in the crossed coefficients represents the contribution of each force X_i with the flux $J_{k \neq i}$. In this case, the parameter q is related to the intrinsic features of the circuit, and can be rewritten in terms of the resistive elements nominal values, as follows:

$$q = \frac{L_{12}}{\sqrt{L_{11} L_{22}}} = \frac{R_2}{\sqrt{\Delta + R_2^2}}, \tag{63}$$

and the force ratio x which has all the extra thermodynamic information of the system, it takes the mathematical expression:

$$x = \sqrt{\frac{L_{11}}{L_{22}}} \frac{X_1}{X_2} = \sqrt{\frac{R_2 + R_3}{R_1 + R_2}} \frac{X_1}{X_2}. \tag{64}$$

In the following, we will study every optimization criteria in terms of arbitrary values that the resistors can adopt, with the aim not only of characterizing the steady state related

21

to an optimal coupling in the circuit stable configuration, but also of ensuring the system adapts to the selected operating regime.

B. Steady state of minimum dissipation function (mdf)

From the mdf–**THEOREM** it follows that x_{mdf} can be rewritten by replacing Eq. (63) in Eq. (64), as

$$x_{mdf} = -\frac{R_2}{\sqrt{\Delta + R_2^2}}, \tag{65}$$

then, the force X_1 is rewritten in this regime as:

$$X_1^{mdf} = -\frac{R_2}{R_2 + R_3} X_2. \tag{66}$$

Thus, the energetics under mdf operation regime is,

$$\Phi_{mdf} = \frac{T X_2^2}{R_2 + R_3} \tag{67a}$$

$$P_{mdf} = 0 \tag{67b}$$

$$\eta_{mdf} = 0. \tag{67c}$$

C. Steady state of maximum power output (MPO)

By applying the MPO–**THEOREM**, we find that x_{MPO} can be written as:

$$x_{MPO} = -\frac{R_2}{2\sqrt{\Delta + R_2^2}}, \tag{68}$$

thereby, the force X_1 acquires the form

$$X_1^{MPO} = -\frac{R_2}{2(R_2 + R_3)} X_2. \tag{69}$$

The energetics beneath MPO operation regime is:

$$\Phi_{MPO} = \left\{ \frac{4\Delta + R_2^2}{4(R_2 + R_3)\Delta} \right\} T X_2^2 \tag{70a}$$

$$P_{MPO} = \left\{ \frac{R_2^2}{4(R_2 + R_3)\Delta} \right\} T X_2^2 \tag{70b}$$

$$\eta_{MPO} = \frac{R_2^2}{4\Delta + 2R_2^2}. \tag{70c}$$

22

D. Steady state of maximum efficiency $(M\eta)$

By taking the $M\eta$–**THEOREM**, we have $x_{M\eta}$ in terms of the resistors values,

$$x_{M\eta} = -\frac{R_2}{\sqrt{\Delta + R_2^2} + \sqrt{\Delta}}, \tag{71}$$

the force associated with driven flux X_1 takes the form:

$$X_1^{M\eta} = -\frac{R_2}{(R_2 + R_3) + \sqrt{\frac{\Delta}{R_1 + R_2}}} X_2. \tag{72}$$

Therefore, the energetics that results in the $M\eta$ regime,

$$\Phi_{M\eta} = \frac{2TX_2^2}{(R_2 + R_3)\left(1 + \sqrt{\Gamma}\right)} \tag{73a}$$

$$P_{M\eta} = \frac{TX_2^2 R_2^2}{\sqrt{(R_2 + R_3)(\Delta + R_2^2)\Delta}\left(1 + \sqrt{\Gamma}\right)^2} \tag{73b}$$

$$\eta_{M\eta} = \frac{R_2^2\sqrt{C}}{2\left(1 + \sqrt{\Gamma}\right)(R_1 + R_3) + R_2^2\sqrt{\Gamma}}, \tag{73c}$$

with $\sqrt{\Gamma} = \sqrt{\frac{\Delta}{\Delta + R_2^2}}$.

E. Steady state of maximum ecological function (MEF)

From the MEF–**THEOREM**, it can be shown that x_{MEF} in terms of the circuit elements [Eq. (63)] is,

$$x_{MEF} = -\frac{3R_2}{4\sqrt{\Delta + R_2^2}}, \tag{74}$$

then, the force X_1 associated with the non-spontaneous flux,

$$X_1^{MEF} = -\frac{3R_2}{4(R_2 + R_3)} X_2. \tag{75}$$

In such a way, the energetics corresponding to the MEF regime remains,

$$\Phi_{MEF} = \left\{\frac{16\Delta + R_2^2}{16(R_2 + R_3)\Delta}\right\} TX_2^2 \tag{76a}$$

$$P_{MEF} = \left\{\frac{3R_2^2}{16(R_2 + R_3)\Delta}\right\} TX_2^2 \tag{76b}$$

$$\eta_{MEF} = \frac{3R_2^2}{4\Delta + R_2^2}. \tag{76c}$$

23

F. Steady state of maximum omega function ($M\Omega$)

By using the $M\Omega$–**THEOREM**, it is derived that $x_{M\Omega}$ can also be denoted as

$$x_{M\Omega} = -\frac{R_2 \left(3 + \Gamma + 4\sqrt{\Gamma}\right)}{4\sqrt{\Delta + R_2^2}\left(1 + \sqrt{\Gamma}\right)^2}, \tag{77}$$

in order to characterize the force X_1,

$$X_1^{M\Omega} = -\frac{R_2 \left(3 + \Gamma + 4\sqrt{\Gamma}\right)}{4 \left(R_2 + R_3\right)\left(1 + \sqrt{\Gamma}\right)^2} X_2 \tag{78}$$

Thus, the energetics is evaluated in the $M\Omega$ regime:

$$\Phi_{M\Omega} = \frac{(R_1 + R_2)\, T X_2^2}{\Delta}\left\{\sqrt{\Gamma} + (1 - \Gamma)\left[\frac{\left(3 + \Gamma + 4\sqrt{\Gamma}\right)^2}{16\left(1 + \sqrt{\Gamma}\right)^4} - \frac{1}{2}\right]\right\} \tag{79a}$$

$$P_{M\Omega} = \frac{T X_2^2 R_2^2 \left(3 + \Gamma + 4\sqrt{\Gamma}\right)\left(1 + 3\Gamma + 4\sqrt{\Gamma}\right)}{16\left(R_2 + R_3\right)\Delta\left(1 + \sqrt{\Gamma}\right)^4} \tag{79b}$$

$$\eta_{M\Omega} = \frac{R_2^2 \left(3 + \Gamma + 4\sqrt{\Gamma}\right)\left(1 + 3\Gamma + 4\sqrt{\Gamma}\right)}{8\left(\Delta + R_2^2\right)\left(1 + \sqrt{\Gamma}\right)^4 \left[1 + \Gamma - \sqrt{\Gamma}\right]}. \tag{79c}$$

G. Steady state of maximum efficient power ($MP\eta$)

Finally, by means of the **MPη–THEOREM**, the forces ratio $x_{MP\eta}$ can be rewritten by using Eq. (63),

$$x_{MP\eta} = -\frac{5 - \Gamma - \sqrt{16\Gamma + (1 - \Gamma)^2}}{6q}, \tag{80}$$

from which it is obtained that X_1 is,

$$X_1^{MP\eta} = -\frac{(R_1 + R_2)\left[5 - \Gamma - \sqrt{16\Gamma + (1 - \Gamma)^2}\right]}{6R_2} X_2. \tag{81}$$

24

Accordingly, the energetics of the system in the $MP\eta$ regime,

$$\Phi_{MP\eta} = \frac{(R_1 + R_2)\,TX_2^2}{\Delta}\left\{1 + \frac{(\Delta + R_2^2)\left[5 - \Gamma - \sqrt{16\Gamma + (1-\Gamma)^2}\right]^2}{36R_2^2} - \frac{\left[5 - \Gamma - \sqrt{16\Gamma + (1-\Gamma)^2}\right]}{3}\right\} \tag{82a}$$

$$P_{MP\eta} = \frac{TX_2^2\,(R_1 + R_2)\left[5 - \Gamma - \sqrt{16\Gamma + (1-\Gamma)^2}\right]\left[6R_2^2 + \Delta\left(\sqrt{16\Gamma + (1-\Gamma)^2}\right) - 4\right]}{36R_2^2\Delta} \tag{82b}$$

$$\eta_{MP\eta} = \frac{\left[5 - \Gamma - \sqrt{16\Gamma + (1-\Gamma)^2}\right]\left[6R_2^2 + \Delta\left(\sqrt{16\Gamma + (1-\Gamma)^2}\right) - 4\right]}{6R_2^2\left[1 + \Gamma + \sqrt{16\Gamma + (1-\Gamma)^2}\right]}. \tag{82c}$$

V. EXPERIMENTAL VERIFICATION OF THE THEORETICAL ENERGETIC HIERARCHY FOR A (2×2)–ELECTRIC CIRCUIT

Just as the steady state characterized by Prigogine is associated with the production of entropy at a minimum and constant rate in a system, it also represents the only thermodynamic state whose useful energy to perform work against the surroundings is zero. When we make a distinction between spontaneous and non-spontaneous processes, we can introduce one more constraint to the system that is related to the extra thermodynamic conditions (operation modes). Then, all of existing steady states bounded between the maximum power output regime and the minimum dissipation regime (minimum entropy production), can be physically attainable.

The validity of the energy conversion theorems as well as their corollaries enunciated and developed in Section 3, is proved through the electric model with resistors previously proposed. Taking into account the operating conditions imposed by the well-known operating regimes (mdf, MPO, $M\eta$, MEF, $M\Omega$ and $MP\eta$), we measure the electric current (driven flux J_1) in mesh 1 of the scheme (see Fig. 4) to reproduce the hierarchical behavior described in Section 2. That is, we are looking for the energetics of the system for different values of the resistor R_2 and, by transitivity for different values of q that always guarantee: $X_1^{mdf} < X_1^{M\eta} < X_1^{MEF} < X_1^{M\Omega} < X_1^{MP\eta} < X_1^{MPO}$.

The nominal resistance values R_2 were calculated to check the existence of the optimal operation regimes, by considering 10 different values of $q \in [0.950, 0.995]$, taken in steps of 0.05. This interval is used in analogy to the results reported by Stucki [16], in which he

25

TABLE II. Resistor R_i and phenomenological coefficients L_{jk} values that correspond to each of the given q values.

q	R_1 (Ω)	R_2 (Ω)	R_3 (Ω)	L_{11} (Ω^{-1})	L_{12} (Ω^{-1})	L_{22} (Ω^{-1})
0.950	100	1900.00	100	0.005128	0.00487	0.005128
0.955	100	2122.22	100	0.005115	0.00488	0.005115
0.960	100	2400.00	100	0.005102	0.00489	0.005102
0.965	100	2757.14	100	0.005008	0.00491	0.005008
0.970	100	3233.33	100	0.005007	0.00492	0.005007
0.975	100	3900.00	100	0.005006	0.00493	0.005006
0.980	100	4900.00	100	0.005005	0.00494	0.005005
0.985	100	6566.67	100	0.005003	0.00496	0.005003
0.990	100	9900.00	100	0.005002	0.00497	0.005002
0.995	100	19900.00	100	0.005001	0.00498	0.005001

considered that values of $q \in [0.95, 0.97]$ show the optimal economic degrees of coupling. For this reason R_1 and R_3 were fixed at a constant value of 100Ω. By using Eq. (63), we estimated the R_2 values for each q.

The next thing was to consider the triad of values for resistors R_1, R_2, and R_3 (see Tab. II), and a fixed value of $X_2 = 12\,\text{V}$ for the DC voltage source related to the driver flux with the purpose of having completely characterized the steady states. From Eqs. (66), (69), (72), (75), (78) and (81), the values of X_1 were found as a function of any operation mode. Thus, with the values of the resistors R_i and the adjusted values for the DC voltage sources X_k, the assembled electric circuit was put inside a container with dielectric oil to emulate its conditions as an isothermal energy converter and, then measure the values of the driven and driver fluxes (electric currents), by considering an enough relaxation time each 5 min approximately to guarantee their stability (steady states).

In Fig. 5, we display the theoretical and experimental trend that the voltage source X_1, as well as the electron fluxes J_1 and J_2 present, according to the operating regimes. In the case of X_1 values, they have as upper bound $X_2 = 12V$ (the value of the fixed force). It is important to note that X_1 values in MP regime, are almost halved with respect to X_2. The purpose of the above-mentioned graphs (Fig. 5) is to compare the behavior of (J_1, J_2, X_1)
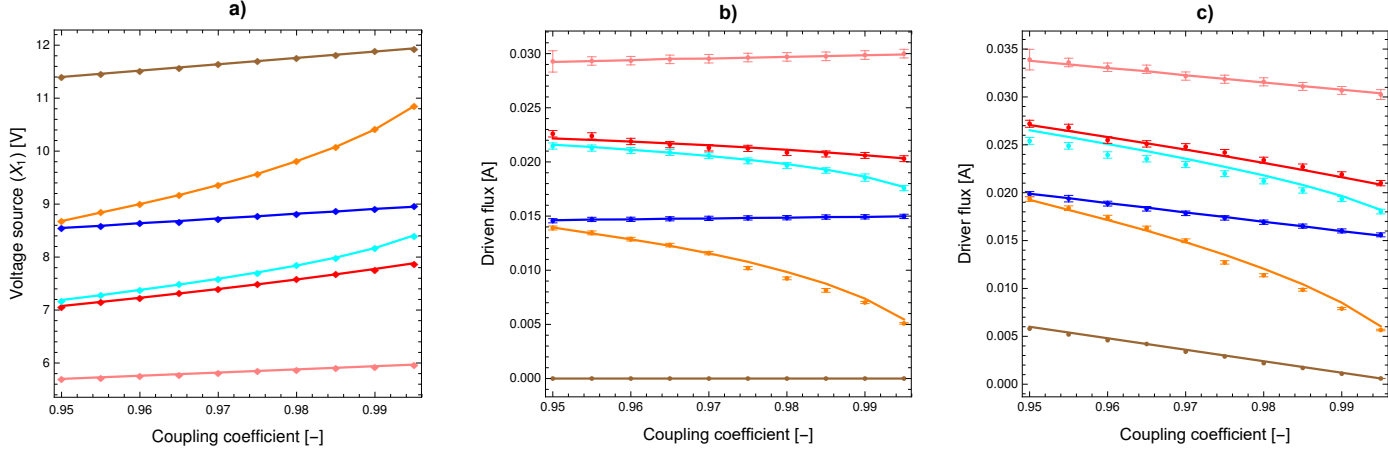
FIG. 5. Graphs of X_1 (source voltage), J_1 (driven flux) and J_2 vs q. All of the points associated with the experimental measurements are shown in diamonds while theoretical models are depicted by solid lines. In a) a hierarchy between the different values of X_1 is displayed. In b) and c) there is also a trend between the operation regimes, they are expressed as the energy consumption in each mesh. The color code for MPO, $MP\eta$, $M\Omega$, MEF, $M\eta$ and mdf are: pink, red, cyan, blue, orange and brown, respectively.

that the linear energy converter model predicts with direct measurements of electric current and voltages through a digital multimeter.

The percentage errors in the measurements for every process variable can be estimated. In the case of power output, the maximum percentage error is calculated for the $M\eta$ regime, its average is $\langle \Delta P_\%^{M\eta} \rangle \approx 6.18\%$. The efficiency presents a maximum mean percentage error when the system works in the $M\Omega$ regime, which is $\langle \Delta \eta_\%^{M\Omega} \rangle \approx 2.75\%$. Finally, dissipation function have the same maximum error in the $M\Omega$ regime, whose value is $\langle \Delta \Phi_\%^{M\Omega} \rangle \approx 7.98\%$. In general, the foregoing shows that the fluctuations produced by the disturbance of the system (interaction with the measuring instruments) are small. This fact guarantees the electric circuit reaches a steady state.

Finally, in Fig. 6 the behavior predicted by theorems enunciated in Section 3 is depicted for the three process variables. Thus, all of physically attainable operation modes for an isothermal linear energy converter are bounded between the maximum power output and minimum dissipation function regimes, while the optimum operation ones lies between the maximum power output and the maximum efficiency regimes.
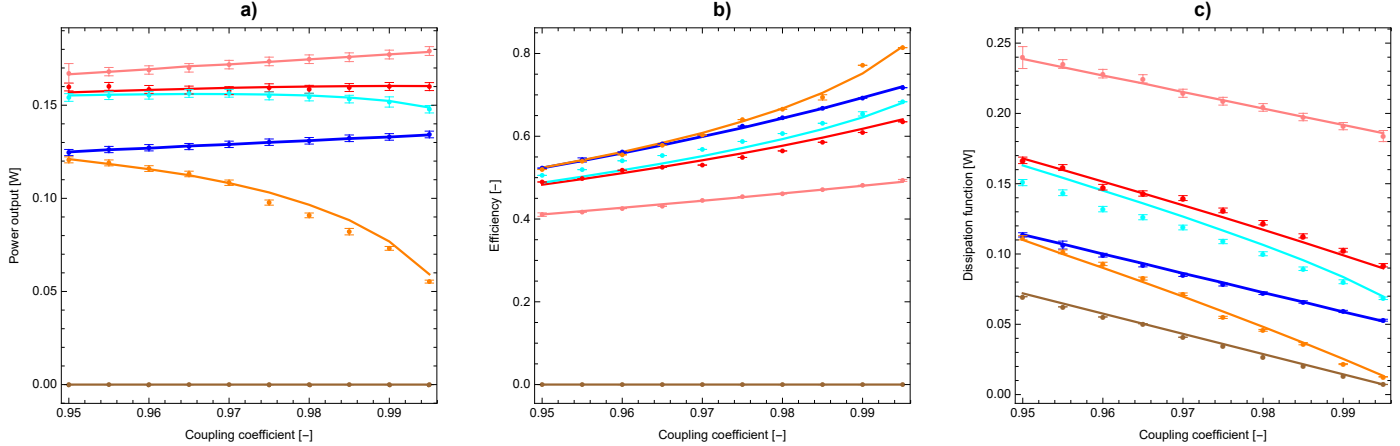
27

FIG. 6. Graphs of the three process variables vs q. All of the points that correspond to the experimental measurements are shown (in diamonds) for a) power output, b) efficiency and c) dissipation function, while the trend given by the theoretical models are depicted in solid lines. The color code for MPO, $MP\eta$, $M\Omega$, MEF, $M\eta$ and mdf are: pink, red, cyan, blue, orange and brown, respectively.

VI. CONCLUSIONS

The whole set of phenomena that can be described by the so-called steady states, few of them have simple uncoupled processes, i.e, a large number of phenomena have the characteristic of being spontaneous and non-interacting. In fact, living and man-made systems characterized by a single process could be said to undoubtedly satisfy Prigogine's theorem.

There is a divided opinion on the validity of the Minimum Entropy Production Theorem and the Principle of Maximum Entropy Production, which largely explain all the processes that occur near of the equilibrium state. In our opinion, if it is desired to obtain a useful energy available through certain coupled processes (energy conversion), and that can be modeled to a large extent by means of so-called energy converters within the context of LIT, then it cannot be expected a minimum entropy production. Furthermore, we have established optimization criteria that are associated with characteristic steady states, which are delimited between the MPO (maximum entropy production) and $M\eta$ operation regimes. That is, other energy conversion theorems can be stated as long as the trade-off between the process variables of the energy converter is well specified.

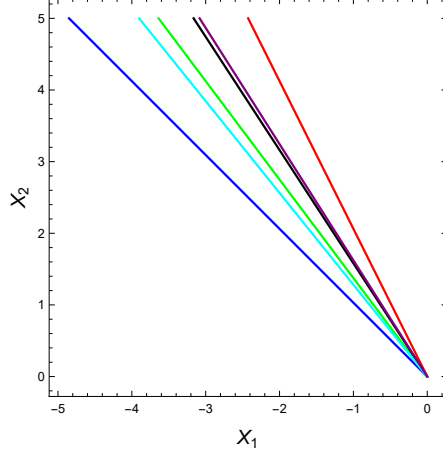In the simple experiment that was designed, we show on the one hand, that the way

28

FIG. 7. Graphic sketch of the proper sub-space $H_{(X1,X2)}$ the for different values of A', X_1 and X_2 are the so-called generalized thermodynamic forces. An order is noted for the 6 operation regimes, *mdf* in blue, *Mη* in cyan, *MEF* in green, *MΩ* in black, *MPη* in purple and *MPO* in red. All lines were depicted under the normalization condition $A' = {}^{A\sqrt{L_{11}}}/\sqrt{L_{22}}$ and with $q = 0.97$.

in which voltage sources (thermodynamic forces) are tuned, lead us to establish a unique performance and on the other hand, that the steady states associated with an energetic objective function are physically accessible. Furthermore, the state described by the minimum entropy production leads us to a zero energy conversion.

ACKNOWLEDGMENTS

Appendix A: Some algebraic properties of the optimal performance regimes

From entropy production definition as a function of the spontaneous and non–spontaneous forces, the surface Φ characterized by an ordered pair (X_1, X_2), lead us to define a vector space given by the basis vectors $\mathcal{X} = \{(X_1, 0), (0, X_2)\}$. Besides, as it is possible to express

X_1 as a function of X_2, then

$$H_{(X1,X2)} := \{(X_1, X_2) | X_1 = AX_2, \text{ with}$$

$$A \text{ a fixed and } X_2 \text{ an arbitrary } \in \Re\}$$

defines the proper subspace of such vector space [59]. An energy converter delimits the vector space of these linear irreversible processes in the region with $X_1 < 0$ and $X_2 > 0$. From Eqs. (4) and (6), we note that these optimal operation modes lie in the subspace $H_{(X1,X2)}$. That is, according to the physical information of A, a linear energy converter can access different physical realizations as long as the thermodynamic forces are tuned under the respective constraints.

Since the restriction $X_1^Y = A^Y X_2$, with Y the optimal operation mode, is associated with a particular extra-thermodynamic condition; in Fig. 7 we can observe the geometric representation of proper sub-spaces of $\mathcal{X}$, restricted to the physical region of linear energy converters given by the Eqs. (4) and (6).

The order displayed in Fig. 7 for each operating regime, can be viewed as the availability of a linear energy converter to locate physical realizations when thermodynamic forces are associated in such a way as to achieve a particular goal in energy conversion. That is, if we measure the distance between an arbitrary point (X_1, X_2) and the equilibrium state $(0, 0)$ for each proper subspace,

$$d(\vec{0}, \vec{X}) = ||\vec{X} - \vec{0}|| = X_2 \sqrt{1 + (A^Y)^2},$$

we observe that $A^{MPO} < A^{MP\eta} < A^{M\Omega} < A^{MEF} < A^{M\eta} < A^{mdf}$ and therefore the distances revels the same order as inequalities [see Eq. (7)].

---

[1] I. Prigogine, *Etude thermodynamique des phénomènes irréversibles*, 1st ed. (Desoer, Liège, 1947) (in French).

[2] R. J. Tykodi, *Thermodynamics of Steady States*, 1st ed. (The Macmillan Company, New York, 1967).

[3] E. T. Jaynes, Ann. Rev. Phys. Chem. **31**, 579 (1980).

[4] M. M. Mamedov, Tech. Phys. Lett. **29**, 340 (2003).

[5] L. M. Martyushev, A. S. Nazarova and V. D. Seleznev, J. Phys. A: Math. Theor. **40**, 371 (2007).

[6] V. Bertola and E. Cafaro, Int. J. Heat Mass Tran. **51**, 1907 (2008).

[7] L. M. Martyushev, Entropy **15**, 1152 (2013).

[8] L. Onsager, Phys. Rev. **37**, 405 (1931).

[9] D. Kondepudi, and I. Prigogine, *Modern Thermodynamics: From Heat Engines to Dissipative Structures*, 1st. ed. (John Wiley & Sons, Chichester, 1998).

[10] I. Ràfols and J. Ortín, Am. J. Phys. **60**, 846 (1992).

[11] I. Danielewicz-Ferchmin and A. Ryszard Ferchmin, Am. J. Phys. **68**, 962 (2000).

[12] D. Lurié and J. Wagensberg, Am. J. Phys. **48**, 868 (1960).

[13] M. J. Klein and P. H. E. Meijer, Phys. Rev. **96**, 250 (1954).

[14] H. B. Callen, *Thermodynamics and an Introduction to Thermostatistics*, 2nd ed. (John Wiley & Sons, New York, 1985).

[15] F. Mandl, *Statistical Physics*, 2nd ed. (John Wiley & Sons, Manchester, 1991).

[16] J. W. Stucki, Eur. J. Biochem. **109**, 269 (1980).

[17] S. R. Caplan, and A. Essig *Bioenergetics and Linear Nonequilibrium Thermodynamics*, 1st ed. (Harvard University Press, Cambridge, 1983).

[18] L. A. Arias–Hernandez, F. Angulo–Brown, and R. T. Paez–Hernandez, Phys. Rev. E **77**, 011123 (2008).

[19] F. Angulo–Brown, M. Santillán, and E. Calleja–Quevedo, Nuovo Cimento Soc. It. Fis. D **17**, 87 (1995).

[20] M. Santillán, L. A. Arias–Hernandez, and F. Angulo–Brown, Nuovo Cimento Soc. Ital. Fis. D **19**, 99 (1997).

[21] L. Onsager, Phys. Rev. **38**, 2265 (1931).

[22] H. B. Callen, Phys. Rev. **73** 1349 (1948).

[23] H. T. Odum and R. C. Pinkerton, Am. Sci. **43**, 331 (1955).

[24] A. Fronczak, P. Fronczak and J. A. Holyst, Phys. Rev. E **76**, 061106 (2007).

[25] M. V. Volkenstein *General Biophysics*, 1st. ed. (Academic Press, London, 1983).

[26] G. Valencia–Ortega and L. A. Arias–Hernandez, J. Non–Equilib. Thermodyn. **42**, 187 (2017).

[27] S. Gonzalez–Hernandez and L. A. Arias–Hernandez, J. Non–Equilib. Thermodyn. **44**, 315 (2019).

[28] G. Valencia–Ortega and L. A. Arias–Hernandez, Physica E **124**, 114231 (2020).

[29] S. R. de Groot, and P. Mazur *Non-Equilibrium Thermodynamics*, 1st. ed. (North-Holland, Amsterdam, 1962).

[30] I. Prigogine *Thermodynamics of Irreversible Processes*, 1st. ed. (Wiley-Interscience, New York, 1967).

[31] L. García–Colín, and P. Goldstein–Menache *Procesos Irreversibles: Teoría y Aplicaciones*, Vol. 1, 1st. ed. (El Colegio Nacional, Mexico City, 2013) (in Spanish).

[32] A. Calvo Hernández, A. Medina, J. M. M. Roco, J. A. White, and S. Velasco, Phys. Rev. E **63**, 037102 (2001).

[33] F. Angulo–Brown, J. Appl. Phys. **69**, 7465, (1991).

[34] T. Yilmaz, J. Energy Inst. **79**, 38, (2006).

[35] L. Chen, and F. Sun *Advances in Finite Time Thermodynamics: Analysis and Optimization*, 1st ed. (Nova Science, New York, 2004).

[36] C. Martinez–Garcia, Master thesis, Instituto Politécnico Nacional (2008) (in Spanish).

[37] Y. Apertet, H. Ouerdane, C. Goupil and Ph. Lecoeur, Phys. Rev. E **88**, 022137 (2013).

[38] J. M. Gordon, and M. Huleihil, J. Appl. Phys. **72**, 829, (1992).

[39] S. Levario–Medina, G. Valencia–Ortega, and M. A. Barranco–Jiménez, J. Non–Equilib. Thermodyn. **45**, 269 (2020).

[40] D. G. Miller, Chem. Rev. **60**, 15 (1960).

[41] H. J. M. Hanley, J. Macromol. Sci. B **3**, 365 (1969).

[42] M. Tribus, *Thermostatics and Thermodynamics*, 1st. ed. (Van Nostrand, Princeton, 1961).

[43] P. Županović, D. Juretić, and S. Botrić, Phys. Rev. E **70**, 056108 (2004).

[44] S. Sasa, and H. Tasaki, J. Stat. Phys. **125**, 125 (2006).

[45] O. Kedem and S. R. Caplan, Trans. Faraday Soc. **21**, 1897 (1965).

[46] F. Angulo–Brown, L.A. Arias–Hernandez, and M. Santillán, Rev. Mex. Fis. **48**, 182, (2002).

[47] V. M. Castillo, Wm. G. Hoover, and C. G. Hoover, Phys Rev. E **55**, 5546 (1997).

[48] Wm. G. Hoover, Am. J. Phys. **70**, 452 (2002).

[49] M. Santillán, G. Maya, and F. Angulo-Brown, J. Phys D: Appl. Phys. **34**, 2068 (2001).

[50] L. Guzmán–Vargas, I. Reyes–Ramírez, and N. Sánchez, J. Phys. D: Appl. Phys. **38**, 1282 (2005).

[51] Y. Huang, and D. Sun, J. Non-Equilib. Thermodyn, **33**, 61 (2008).

[52] P.A.N. Wouagfack, and G. Keune, Int. J. Refrig. **65**, 38 (2017).

[53] J. González-Ayala, J. Guo, A. Medina, J.M.M. Roco, and A. Calvo Hernández, Phys. Rev. Lett. **124**, 050603 (2020).

[54] J. S. Lee, J. M. Park, H. M. Chun, J. Um and H. Park, Phys. Rev. E **101**, 052132 (2020).

[55] G. Valencia-Ortega, S. Levario-Medina, and M.A. Barranco-Jiménez, Physica A **571**, 125863 (2021).

[56] P. Glansdorff, and I. Prigogine, Physica, **20**, 773 (1954).

[57] P. Glansdorff, and I. Prigogine, *Thermodynamic Theory of Structure, Stability and Fluctuations*, 1st. ed. (Wiley–Interscience, London, 1971).

[58] G. Nicolis, and I. Prigogine, *Self-organization in nonequilibrium systems*, 1st. ed. (John Wiley & Sons, New York, 1977).

[59] S.I. Grossman, *Elementary Linear Algebra*, 5th. ed. (Thomson Learning, Stamford, 1994).